2015-06-03

Functional Upregulation of alpha4* Nicotinic Acetylcholine Receptors in VTA GABAergic Neurons Increases Sensitivity to Nicotine Reward

Jennifer Ngolab
University of Massachusetts Medical School

Et al.

Behavioral/Cognitive

Functional Upregulation of α4* Nicotinic Acetylcholine Receptors in VTA GABAergic Neurons Increases Sensitivity to Nicotine Reward

Jennifer Ngolab,[1] Liwang Liu,[1] Rubing Zhao-Shea,[1] Guangping Gao,[2,3] Paul D. Gardner,[1] and Andrew R. Tapper[1]

[1]Brudnick Neuropsychiatric Research Institute, Department of Psychiatry and [2]Gene Therapy Center, [3]Department of Microbiology and Physiological Systems, University of Massachusetts Medical School, Worcester, Massachusetts 01604

Chronic nicotine exposure increases sensitivity to nicotine reward during a withdrawal period, which may facilitate relapse in abstinent smokers, yet the molecular neuroadaptation(s) that contribute to this phenomenon are unknown. Interestingly, chronic nicotine use induces functional upregulation of nicotinic acetylcholine receptors (nAChRs) in the mesocorticolimbic reward pathway potentially linking upregulation to increased drug sensitivity. In the ventral tegmental area (VTA), functional upregulation of nAChRs containing the α4 subunit (α4* nAChRs) is restricted to GABAergic neurons. To test the hypothesis that increased functional expression of α4* nAChRs in these neurons modulates nicotine reward behaviors, we engineered a Cre recombinase-dependent gene expression system to selectively express α4 nAChR subunits harboring a "gain-of-function" mutation [a leucine mutated to a serine residue at the 9′ position (Leu9′Ser)] in VTA GABAergic neurons of adult mice. In mice expressing Leu9′Ser α4 nAChR subunits in VTA GABAergic neurons (Gad2^{VTA}:Leu9′Ser mice), subreward threshold doses of nicotine were sufficient to selectively activate VTA GABAergic neurons and elicit acute hypolocomotion, with subsequent nicotine exposures eliciting tolerance to this effect, compared to control animals. In the conditioned place preference procedure, nicotine was sufficient to condition a significant place preference in Gad2^{VTA}:Leu9′Ser mice at low nicotine doses that failed to condition control animals. Together, these data indicate that functional upregulation of α4* nAChRs in VTA GABAergic neurons confers increased sensitivity to nicotine reward and points to nAChR subtypes specifically expressed in GABAergic VTA neurons as molecular targets for smoking cessation therapeutics.

Key words: **GABA; nicotine; nicotinic receptor; reward**

Introduction

Chronic exposure to tobacco smoke accounts for ~5 million deaths per year, making health complications from smoking the primary cause of preventable mortality in the world (Harris and Anthenelli, 2005). Nicotine, the addictive component of tobacco, binds to and activates neuronal nicotinic acetylcholine receptors (nAChRs), ligand-gated cation channels that are normally activated by the endogenous neurotransmitter, acetylcholine (ACh). Nicotine initiates dependence by activating neurons within the ventral tegmental area (VTA) of the mesocorticolimbic reward circuitry, ultimately driving the release of dopamine (DA) within the nucleus accumbens (NAc), a phenomenon widely associated with the rewarding or reinforcing value of nicotine (De Biasi and Dani, 2011). A large variety of nAChR subunit genes are expressed in both VTA DAergic projection neurons and GABAergic neurons (Klink et al., 2001; Wooltorton et al., 2003).

Neuronal nAChRs are pentameric receptors consisting of homologous or heterologous combinations of subunits. Twelve genes encoding 12 individual nAChR subunits have been identified, accounting for a vast array of nAChR subtypes each with distinct pharmacological and biophysical properties. A great deal of effort has focused on identifying nAChR subtype expression within the VTA to determine which subtypes, when activated, are necessary and sufficient for nicotine reinforcement and/or reward (Picciotto et al., 1998; Tapper et al., 2004; Maskos et al., 2005; Pons et al., 2008). From these studies, a general consensus is that expression of nAChRs containing α4 and β2 subunits in the VTA are both necessary and sufficient for nicotine reinforcement with at least some contribution of the α6 subunit (Pons et al., 2008; Brunzell et al., 2010; Gotti et al., 2010). However, α4 and β2 subunits are expressed in both VTA DAergic neurons and GABAergic neurons (Klink et al., 2001; Wooltorton et al., 2003). Although nicotine can directly activate VTA DAergic neurons, previous studies suggest that activation of GABAergic neurons may also modulate DAergic neuron activity and is required for nicotine reinforcement (Tolu et al., 2012).

Unlike other drugs of abuse, chronic use of nicotine leads to increased expression or "upregulation" of α4β2* nAChRs (the

Received Oct. 27, 2014; revised April 27, 2015; accepted April 29, 2015.

Author contributions: J.N., L.L., R.Z.-S., G.G., P.D.G., and A.R.T. designed research; J.N., L.L., and R.Z.-S. performed research; J.N., L.L., R.Z.-S., G.G., P.D.G., and A.R.T. analyzed data; J.N., P.D.G., and A.R.T. wrote the paper.

This work was supported by Awards F31DA034490 (J.N.) and R21DA036041 (A.R.T.) from the National Institute on Drug Abuse. We thank Karl Deisseroth for the AAV-Ef1A-DIO-ChR2-eYFP plasmid. The content is solely the responsibility of the authors and does not necessarily represent the official views of the National Institutes of Health.

The authors declare no competing financial interests.

Correspondence should be addressed to Dr. Andrew R. Tapper, University of Massachusetts Medical School, 303 Belmont Street, Worcester, MA 01604. E-mail: andrew.tapper@umassmed.edu.

DOI:10.1523/JNEUROSCI.4453-14.2015

 0270-6474/15/358570-09$15.00/0

asterisk denotes that nAChR subunits in addition to α4 and β2 may be assembled in the nAChR complex) in the mesocorticolimbic pathways in addition to other brain regions. Although upregulation of nAChRs is a hallmark of chronic nicotine exposure, the behavioral consequence of this phenomenon and how it relates to nicotine dependence is unknown (Wonnacott, 1990). Interestingly, functional upregulation of α4* nAChRs in the mesolimbic pathway appears to be restricted to midbrain GABAergic neurons including those of the VTA (Nashmi et al., 2007; Xiao et al., 2009). In addition, the rewarding properties of nicotine have been shown to increase in chronic nicotine-exposed mice, perhaps linking upregulation and increased functional α4* nAChR expression in VTA GABAergic neurons with reward behavior (Hilario et al., 2012). We sought to test the hypothesis that increased functional expression of α4* nAChRs selectively in VTA GABAergic neurons will increase sensitivity to nicotine reward.

Materials and Methods

Mice. C57BL/6J and glutamate decarboxylase 2 (Gad2)-Cre (strain *B6N.Cg-Gad2$^{tmz(cre)Zhj}$/J*) male mice on a C57BL/6J background were used in this study (The Jackson Laboratory; Taniguchi et al., 2011). Adult (8 to 10 weeks old) Gad2-Cre mice were injected with viral particles and used for behavioral experiments 4–6 weeks after infection. All mice were kept on a 12 h light/dark cycle, with lights on at 7:00 A.M. and off at 7:00 P.M. All mice were given food and water *ad libitum*. All procedures were performed in compliance with the Institutional Animal Care and Use Committee of the University of Massachusetts Medical School.

Drugs. For acute treatments, nicotine hydrogen tartrate, mecamylamine hydrocholoride (Sigma-Aldrich), and dihydro-β-erythroidine hydrobromide (DHβE; Tocris Bioscience) were dissolved in sterile 0.9% PBS (Hospira). Nicotine was titrated to physiological pH (7.4) before being administered to mice. Vials containing nicotine solutions were wrapped in aluminum foil to prevent degradation by light exposure. For chronic exposure studies, nicotine dihydrate ditartrate (200 μg/ml; Acros Organics) and L-tartaric acid (300 μg/ml; Sigma-Aldrich) were dissolved in water. Saccharin sodium (3 mg/ml; Fisher Scientific) was added to both solutions to increase palatability. Doses for nicotine, mecamylamine, and DHβE were calculated as free base. All injections were administered subcutaneously.

Viral plasmid engineering. The mouse α4-yellow fluorescent protein (YFP) nAChR subunit cDNA was obtained from Addgene (plasmid 15245) and has been described previously (Nashmi et al. 2003). Using the QuikChange site-directed mutagenesis kit (Agilent Technologies), PCR mutagenesis was done to convert the 9′ leucine of the M2 pore domain to a serine (changing the codon from CTT to TCT). The resulting construct contained α4-YFP cDNA with the leucine to serine mutation (Leu9′Ser α4-YFP). The Leu9′Ser α4-YFP cDNA was subcloned into the AAV expression vector pAAV-EF-1a-DIO-WPRE-pA (Tsai et al., 2009).

Chronic nicotine exposure. Animals were restricted to drinking either control (tartaric acid, 300 μg/ml and 3 mg/ml saccharin) or nicotine-treated (200 μg/ml and 3 mg/ml saccharin) water through a 250 ml opaque water bottle placed in the home cage for 6–8 weeks. To induce withdrawal, the nicotine bottle was replaced with a water bottle (Zhao-Shea et al., 2013).

Viral-mediated gene delivery. Both the pAAV-EF-1a-Leu9′Ser-α4-YFP (Leu9′Ser α4-YFP) and pAAV-EF-1a-DIO-hChR2(H134R)-EYFP-WPRE-pA (control) constructs were packaged into AAV2 viral particles by the University of Massachusetts Medical School Viral Vector Core. Viral titers were 10^{12} viral particles/μl with 1 μl of viral supernatant bilaterally injected into the VTA. Gad2-Cre animals were anesthetized with ketamine/xylazine (0.1 ml/10 g body weight, 10 mg/ml ketamine, 1 mg/ml xylazine). To prepare the surgical area, fur was shaved, and skin was disinfected with 10% povidone iodine. The VTA was located with a stereotaxic frame (Stoelting) using the following coordinates from bregma (in mm): −3.3 AP, ±0.3 ML, −4.0 DV. Viral particles were infused into the brain using an injection syringe (Hamilton) attached to a syringe pump (Quintessential Stereotaxic Injector, Stoelting) at a rate of 0.25 μl/min. The injection needle was left in place for 10 min after each injection and then slowly retracted. Mice were given 5% glucose and 15 mg/kg ketaprofen after fully regaining consciousness. Mice were given 4 weeks for recovery and to allow for expression of the viral particles before each experiment.

Immunofluorescence. For c-Fos immunolabeling, animals received subcutaneous saline injections 3 d before each experiment to reduce possible effects of stress and/or handling on neuronal activity. To assess c-Fos expression, Gad2-Cre male mice infected with either control or Leu9′Ser α4-YFP were injected either with saline or 0.09 mg/kg nicotine. Ninety minutes after drug administration, brains were harvested for slice preparation. Animals were anesthetized with 200 mg/kg sodium pentobarbital (interperitoneal injection) and transcardially infused with 10 ml of chilled 0.1 M PBS following with chilled 4% (w/v) paraformaldehyde dissolved in 0.1 M PBS. The brains were harvested and placed in cold 4% paraformaldehyde for 2 h before submerging in 30% sucrose. Brains were then sectioned into 30 μm slices using a microtome (Leica) and immunolabeled via free-floating sections. Slices were washed in PBS for 5 min, permeabilized in 0.2% (v/v) Triton X-100 (Sigma-Aldrich) for 5 min, and blocked with 2% bovine serum albumin (BSA; Fisher Scientific) for 30 min before incubation with primary antibody in 2% BSA overnight at 4 °C. Primary antibodies used were as follows: mouse anti-TH MAB318 (1:1000; lot number 2499557, Millipore), rabbit anti-Gad1/2 (1:2000; lot number 122M4761, Sigma-Aldrich), rabbit anti-c-Fos (1:1000; lot number F2510, Santa Cruz Biotechnology), rabbit anti-GFP (1:4000; lot number GR158277-1, Abcam), mouse anti-calbindin (1:3000; lot number 052M4833, Sigma-Aldrich), rabbit anti-calretinin (1:1000; lot number AB5054, Millipore), rabbit anti-parvalbumin (1:1000; lot number ab11427, Abcam), and goat anti-somatostatin (1:100; lot number sc-789, Santa Cruz Biotechnology). Secondary antibodies were Alexa Fluor 405 (lot number 1126599), 488 (lot number 1608521), and 594 (lot numbers 1431805, 1003216, and 1602780; 1:1000; Invitrogen). An AxioCam MRm camera (Carl Zeiss) attached to a Zeiss Axiovert inverted fluorescent microscope equipped with Zeiss filter sets 38HE, 49, and 20 was used to acquire fluorescent images. Zeiss objectives A-plan 10×, EC-Plan-NEOFLUAR 20×, and Plan-APOCHROMAT 63× were used to view and capture images. Images were processed using Axiovision version 4.8.2. For quantification and colocalization analysis, images were deconvoluted and segmented using the segmentation and quantification of subcellular shapes (Squassh) software plugin through ImageJ. At least 10 slices/mouse brain that spanned the entire VTA were analyzed. The VTA was located using TH staining and morphology of nearby brain regions as described previously (Zhao-Shea et al., 2011). Areas of interest for each slice were identified through TH fluorescence and measured in ImageJ using the "Analyze Particles" option to account for differences between slices.

Electrophysiological recordings. Mice were deeply anesthetized with sodium pentobarbital (200 mg/kg, i.p.) and then decapitated. Slices were prepared as described previously (Zhao-Shea et al., 2011). Briefly, brains were quickly removed and placed in an oxygenated ice-cold high sucrose artificial CSF (SACSF) containing kynurenic acid (1 mM; Sigma-Aldrich). Brain slices (180–200 μm) were cut using a Leica VT1200 vibratome. The brain slices were incubated in oxygenated Earl's balanced salt solution supplemented with glutathione (1.5 mg/ml; Sigma), *N*-ω-nitro-L-arginine methyl ester hydrochloride (2.2 mg/ml; Sigma), pyruvic acid (11 mg/ml; Sigma), and kynurenic acid (1 mM) for 45 min at 34°C. Slices were transferred into oxygenated ACSF at room temperature for recording. SACSF solution contained the following (in mM): 250 sucrose, 2.5 KCl, 1.2 $NaH_2PO_4 \cdot H_2O$, 1.2 $MgCl_2 \cdot 6\ H_2O$, 2.4 $CaCl_2 \cdot 2\ H_2O$, 26 $NaHCO_3$, 11 D-glucose. Single slices were transferred into a recording chamber continually superfused with oxygenated ACSF. The junction potential between the patch pipette and bath ACSF was nullified just before obtaining a seal on the neuronal membrane. Action potentials and currents were recorded at 32°C using the whole-cell configuration of a Multiclamp 700B patch-clamp amplifier (Molecular Devices). Action potentials were obtained using a gap-free acquisition mode and Clampex software (Molecular Devices). I_h currents were elicited every 5 s by stepping from −60 mV to a test potential of −120 mV for 1 s using Clampex.

Table 1. Total time spent (in seconds) in drug- and saline-paired chambers of the CPP assay before (Pre) and after (Post) training

	Sal (Pre, s)	Sal (Post, s)	Drug (Pre, s)	Drug (Post, s)
Virus (Nic, mg/kg)				
Ctrl (Sal)	379.7 ± 20.86	315.7 ± 48.44	280.2 ± 18.88	335.5 ± 45.96
Ctrl (0.09)	339 ± 9.444	309.3 ± 47.33	271.1 ± 14.35	249.5 ± 45.42
Ctrl (0.5)	334.9 ± 32.69	341.1 ± 21.41	284.9 ± 17.82	299.3 ± 24.08
Leu9′Ser (Sal)	365.6 ± 25.91	315.6 ± 53.89	261.7 ± 21.01	239.0-±34.97
Leu9′Ser (0.09)	347.6 ± 21.93	205.9 ± 27.43	257.1 ± 17.7	437.9 ± 37.28**,^
Leu9′Ser (0.5)	303.3 ± 24.92	240.4 ± 18.14	293 ± 13.92	319.2 ± 37.3
Leu9′Ser (0.5, chronic nicotine)	382 ± 10.11	294.1 ± 19.78	306.8 ± 16.57	376.1 ± 19.33*,^
Virus (Mec, mg/kg)				
Ctrl (1.0)	409.2 ± 28.42	352.5 ± 40.04	282.3 ± 29.93	317.6 ± 43.69
Leu9′Ser (1.0)	386.1 ± 25.30	300.1 ± 36.56	288.2 ± 23.48	354.0 ± 35.28
Virus (DHβE, mg/kg)				
Ctrl (0.5)	363.8 ± 31.05	342.9 ± 24.21	311.7 ± 30.39	315.1 ± 22.15
Ctrl (2.0)	447.6 ± 31.12	332.2 ± 38.96	226.3 ± 32.76	285.9 ± 44.42
Leu9′Ser (0.5)	396.1 ± 23.09	287.7 ± 41.97	244 ± 22.59	348.2 ± 41.85
Leu9′Ser (2.0)	383.1 ± 16.36	352 ± 55.83	309.4 ± 12.95	309.6 ± 55.02
Treatment/drug				
Control/nicotine	367 ± 20.3	328.5 ± 23.48	268.8 ± 18.67	263.7 ± 26.09
Chronic nicotine/nicotine	400.2 ± 29.79	263.2 ± 23.39	261.1 ± 15.01	379.6 ± 26.02*,#

Ctrl, Control; Nic, nicotine; Sal, saline; Mec, mecamylamine.

*$p < 0.05$; **$p < 0.01$ [post-training compared to pretraining, two-way ANOVA with repeated measures (training and nicotine/saline treatment) and Bonferroni's *post hoc* test].

#$p < 0.01$ [time spent in the nicotine-paired chamber after training for nicotine-dependent animals compared to time spent in the nicotine-paired chamber for nicotine-naïve animals; two-way ANOVA with repeated measures (Pre/Post time spent in the Nic-paired chamber) and Bonferroni's *post hoc* test].

^$p < 0.001$ [time spent in the nicotine-paired chamber after training compared to time spent in the control nicotine-paired chamber, i.e., group that received saline in the "drug-paired" chamber; two-way ANOVA with repeated measures (Pre/Post time spent in the Nic-paired chamber) and Bonferroni's *post hoc* test].

Input resistances were calculated using steady state currents elicited by 5 mV hyperpolarizing pulses. Signals were filtered at 1 kHz using the amplifier's four-pole, low-pass Bessel filter, digitized at 10 kHz with an Axon Digidata 1440A interface and stored on a personal computer. Potential VTA GABAergic neurons were selected for recording based on fluorescent signal and further verified by action potential frequency (~10–20 Hz) and lack of I_h expression. At the end of recording, the neuronal cytoplasm was aspirated into the recording pipette, and the contents were expelled into a microcentrifuge tube containing 75% ice-cold ethanol and stored at −20°C for at least 2 h before single-cell RT-PCR experiments to verify expression of GAD1 and GAD2. ACh chloride (Sigma) was dissolved in ACSF. Whole-cell ACh responses were recorded in the presence of TTX (0.5 μM), atropine (1 μM), bicuculline (20 μM), and CNQX (10 μM). Drugs were applied to slices by gravity superfusion.

Nicotine tolerance. Mice received subcutaneous saline injections 3 d before testing to habituate to handling. Locomotor activity was recorded as beam breaks using the Photobeam Activity System (PAS; San Diego Instruments). To determine baseline activity, mice were injected with saline and immediately placed into a novel cage inside the PAS locomotor chamber. Activity was quantified for 15 min before mice were returned to their home cage. On the second day, mice received a subcutaneous injection of nicotine and were immediately placed into a novel cage within the locomotor activity chamber. Activity was measured for 15 min. Mice were subsequently injected with nicotine each day for 6 more days, with locomotor activity recorded on the fourth and seventh days of nicotine challenge.

Conditioned place preference. A three-chamber conditioned place preference (CPP) apparatus (Med Associates) was used to measure nicotine reward. Briefly, at least 3 d before testing, mice were habituated to the test room and handling by picking them up once a day by the scruff of the neck. The testing protocol comprised three phases. In the pretraining phase, mice were placed into the CPP apparatus and allowed to freely explore all three chambers for 15 min. Time spent in each chamber was quantified using MEDPC IV software (Med Associates). The training phase lasted 4 d, where each day mice were twice confined to a chamber for 30 min. In the morning session, each mouse was given a subcutaneous injection of sterile saline and placed in the chamber assigned as the saline-paired chamber. Five hours later, each mouse was given a subcutaneous injection of drug (i.e., nicotine) and placed in the opposite, drug-paired chamber. The training phase was counterbalanced for each group in that approximately half of the animals received nicotine paired with the white chamber, whereas the other half received nicotine paired with the black chamber. Drug was paired with the least preferred chamber. Mice that spent >70% of pretraining in any one chamber were not included in the analysis. The post-training phase was identical to the pretraining phase. Difference scores were measured by calculating the difference between the time spent in a chamber during the post-training phase and during the pretraining phase. For CPP experiments testing nicotine reward in control and Leu9′Ser α4-YFP-infected mice (see Fig. 3, Table 1), the CPP procedure was initiated 4–6 weeks after infection. Mice received saline in both chambers, 0.09 mg/kg nicotine, or 0.5 mg/kg nicotine ($n = 8$–10 mice/group) during training. Additional groups of control and Leu9′Ser α4-YFP-infected mice were tested for CPP to 1 mg/kg mecamylamine ($n = 8$–10 mice/group) or 0.5 or 2.0 mg/kg DHβE ($n = 6$–8 mice/group) as described in Figure 4, *A* and *B*, and Table 1. For this set of experiments, CPP was performed exactly as described above except instead of nicotine during training, mice received mecamylamine or DHβE at the indicated dose. For CPP in nicotine-dependent mice (see Fig. 3*C*, inset; Table 1), mice were exposed to nicotine in their drinking water for 8 weeks. Water bottles were swapped for untreated drinking water after the completion of the CPP pretraining phase, and CPP was performed as above using 0.5 mg/kg nicotine during training ($n = 11$). An additional group of control nicotine-naive animals were also tested in the CPP procedure using 0.5 mg/kg nicotine ($n = 11$).

Statistics. Normality of data was tested before analysis. Locomotor activity data were analyzed using repeated measures one-way ANOVA. CPP data were analyzed using two-way ANOVA with drug dose and paired chamber as main factors, followed by Bonferroni's *post hoc* analysis as indicated. c-Fos data were analyzed using two-way ANOVA with virus and drug treatment or neuron subtype as main factors as indicated. Fold-change differences in inward current were analyzed using a two-tailed *t* test. Data were analyzed using GraphPad Prism (GraphPad Software).

Results

Expression of gain-of-function α4 nicotinic receptor subunits in VTA GABAergic neurons

To understand how increased functional expression of α4* nAChRs in VTA GABAergic neurons affects behavior, we developed a viral-mediated gene delivery system to express α4* nico-

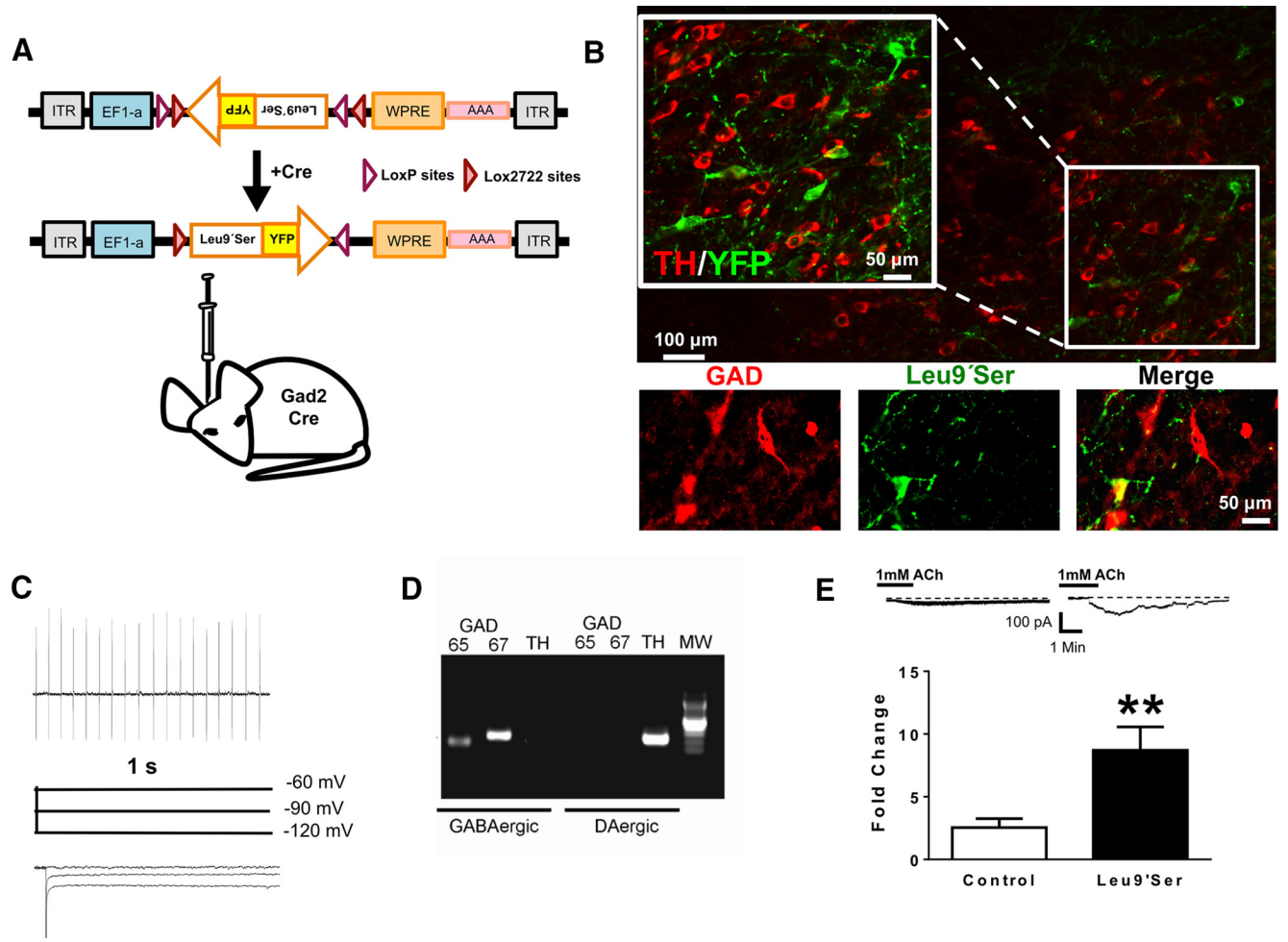

Figure 1. Viral-mediated gene delivery of gain-of-function α4 nAChR subunits in VTA GABAergic neurons. ***A***, Depiction of the Leu9′Ser α4-YFP subunit cDNA viral plasmid. Cre-recombinase flips the Leu9′Ser α4-YFP subunit cDNA in the sense orientation. The viral particles containing this plasmid were intracranially injected into the VTA of Gad2-Cre mice for selective expression in VTA GABAergic neurons. ***B***, Top, Expression of Leu9′Ser α4-YFP subunits in non-TH neurons of Gad2-Cre mice. Brain slices from infected mice were immunolabeled for TH to identify DAergic neurons (red, top, left). YFP fluorescence was detected, indicating Leu9′Ser α4-YFP subunit expression (green, top, middle). Merged signals revealed little colocalization of Leu9′Ser α4-YFP subunit expression with DAergic neurons (top, right). Photomicrographs (bottom) of a representative VTA midbrain section from Gad2-Cre mice expressing Leu9′Ser α4-YFP subunits show neurons immunolabeled for Gad (left) that also express Leu9′Ser α4-YFP subunits (middle). The merged photomicrograph (right) shows colocalization of Gad and YFP signals. ***C***, Cell-attached (top) and whole-cell voltage-clamp (bottom) recordings from a putative VTA GABAergic neuron from a Gad2-Cre mouse midbrain slice. GABAergic neurons typically have a high frequency of firing (8–20 Hz, top) and lack of a hyperpolarizing activated current, I_h (bottom). ***D***, At the end of each recording, single-neuron RT-PCR was performed to verify Gad expression in a GABAergic neuron (left lanes) or TH expression in a DAergic neuron (right lanes). ***E***, Top, Whole-cell voltage-clamp recordings from a control VTA GABAergic neuron in a Gad2-Cre midbrain slice (left) and an Leu9′Ser α4-YFP-expressing GABAergic neuron in a Gad2-Cre midbrain slice (right). ACh was bath applied for 3 min as indicated by the bar above each trace. Average inward current from control infected ($n = 5$) and Leu9′Ser α4-YFP ($n = 8$) infected VTA GABAergic neurons. $^{**}p < 0.01$ (two-tailed t test). Error bars indicate SEM.

tinic receptor subunits with a gain-of-function mutation in select neuronal populations allowing for selective activation of neurons expressing this subunit with low doses of nicotine that minimally activate non-α4* nAChRs. We engineered an AAV plasmid construct containing cDNA encoding the α4 nAChR subunit with a single point mutation, a leucine mutated to serine, at the 9′ residue of the pore-forming, M2 domain (Leu9′Ser; Fig. 1*A*), which renders nAChRs that incorporate this subunit significantly more sensitive to nicotine (Labarca et al., 2001). To visualize subunit expression, a YFP tag was included in the M3–M4 intracellular loop, where it does not interfere with receptor assembly or function (Leu9′Ser α4-YFP; Nashmi et al., 2003; Nashmi et al., 2007). The cDNA encoding Leu9′Ser α4-YFP was positioned within the AAV expression vector in the antisense orientation and flanked by two pairs of distinct Lox sites (Fig. 1*A*). These Lox sites regulate Leu9′Ser α4-YFP expression by directing recombination of the cDNA cassette to the sense orientation in the presence of Cre recombinase (Fig. 1*A*) (Tsai et al., 2009).

The expression vector was packaged into AAV2, a serotype that will infect a brain region locally, and viral particles were injected into the VTA of Gad2-Cre mice (Gad2^{VTA}:Leu9′Ser) for expression of Leu9′Ser α4-YFP subunits selectively in GABAergic neurons. To verify subunit expression in GABAegic neurons, Gad2^{VTA}:Leu9′Ser midbrain slices were immunolabeled with either an anti-TH or Gad1/2 antibody. VTA of infected mice exhibited robust expression of Leu9′Ser α4-YFP subunits, as indicated by strong YFP fluorescent signal selectively in non-DAergic neurons (Fig. 1*B*). To determine functional expression of Leu9′Ser α4-YFP subunits in GABAergic VTA neurons, patch-clamp recordings were made in Gad2^{VTA}:Leu9′Ser and control midbrain slices. Control Gad2-Cre animals were infected with AAV2 particles containing channelrhodopsin within the same vector so that GABAergic neurons from control mice would express a non-nAChR membrane protein insensitive to nicotinic agonists. The electrophysiological characteristics of infected neurons, as identified by YFP fluorescent signal, were analyzed to

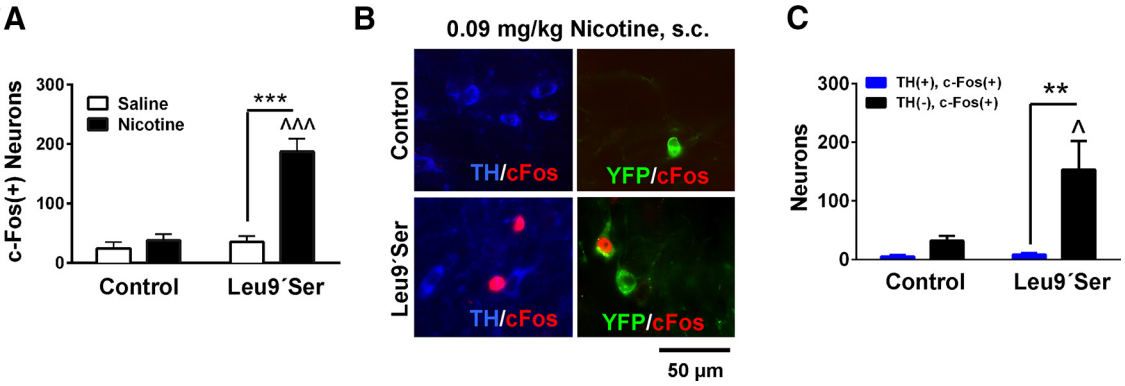

Figure 2. Selective activation of VTA GABAergic neurons by nicotine in Gad2^{VTA}:Leu9′Ser mice. ***A***, Summed average number of c-Fos-immunopositive [c-Fos(+)] neurons in the VTA of control ($n = 6$/group) and Gad2^{VTA}:Leu9′Ser mice ($n = 7$/group) after challenge with saline or 0.09 mg/kg nicotine. ***B***, Representative photomicrographs illustrating c-Fos expression (red) in VTA sections taken from control (top) or Gad2^{VTA}:Leu9′Ser mice (bottom) mice after 0.09 mg/kg nicotine challenge. Neurons exhibiting TH immunoreactivity are labeled in blue (left), whereas YFP expression is labeled in yellow (right). ***C***, Summed average number of TH(+), c-Fos(+) and TH(−), c-Fos(+) neurons in the VTA in control ($n = 6$ mice) and Gad2^{VTA}:Leu9′Ser mice ($n = 7$) after challenge with 0.09 mg/kg nicotine. $^{**}p < 0.01$ [number of TH(+), c-Fos(+) neurons compared to the number of TH(−), c-Fos(+) neurons in Gad2^{VTA}:Leu9′Ser mice after nicotine challenge]; $^{***}p < 0.001$ [number of c-Fos(+) neurons in Gad2^{VTA}:Leu9′Ser mice after nicotine challenge compared to saline challenge]; $^{\wedge} p < 0.05$ [number of neurons that are TH(−), c-Fos(+) in Gad2^{VTA}:Leu9′Ser mice after nicotine challenge compared to the number of neurons that are TH(−), c-Fos(+) in control mice after nicotine challenge]; $^{\wedge\wedge\wedge}p < 0.001$ [number of c-Fos(+) neurons in Gad2^{VTA}:Leu9′Ser mice after nicotine challenge compared to the number of c-Fos(+) neurons in control mice after nicotine challenge]. Error bars indicate SEM.

confirm incorporation of the Leu9′Ser α4-YFP subunit into an nAChR. Leu9′Ser α4-YFP-infected neurons exhibited fast-spiking spontaneous action potentials and lacked an I_h current, both characteristics of VTA GABAergic neurons (Fig. 1*C*; Johnson and North, 1992). Single-cell RT-PCR from the cytoplasm of recorded neurons confirmed Gad1 and Gad2 expression in YFP-positive neurons (Fig. 1*D*). To test for functional expression of the Leu9′Ser α4-YFP subunit, whole-cell current responses to bath application of 1 mM ACh were recorded in infected Gad2-Cre midbrain slices. ACh elicited robust inward currents in Leu9′Ser α4-YFP subunit-expressing VTA GABAergic neurons that were significantly larger compared to responses from neurons recorded from control slices (Fig. 1*E*). Together, these data suggest that Gad2^{VTA}:Leu9′Ser mice express the Leu9′Ser α4-YFP subunit in GABAergic neurons, and the subunit coassembles with endogenous subunits to form gain-of-function nAChRs.

Selective activation of VTA GABAergic neurons in Gad2^{VTA}:Leu9′Ser mice

To test the hypothesis that a low dose of nicotine selectively increased activation of VTA neurons in nicotine-naive Gad2^{VTA}:Leu9′Ser mice compared to control animals, we challenged each group with saline or an acute dose of 0.09 mg/kg nicotine and immunolabeled VTA slices for c-Fos expression, an immediate early gene that is a marker for neuron activation (Cole et al., 1989). Two-way ANOVA indicated a significant main effect of virus expression ($F_{(1,22)} = 29.96$, $p < 0.001$) and nicotine treatment ($F_{(1,22)} = 31.62$, $p < 0.001$), and a significant virus expression by nicotine treatment interaction ($F_{(1,22)} = 22.23$, $p < 0.001$; Fig. 2*A*). *Post hoc* analysis indicated that there was a statistically significant increase of c-Fos-immunopositive VTA neurons from Gad2^{VTA}:Leu9′Ser mice receiving 0.09 mg/kg nicotine compared to Gad2^{VTA}:Leu9′Ser mice receiving saline injection ($p < 0.0001$). In addition, the number of c-Fos-immunopositive VTA neurons in Gad2^{VTA}:Leu9′Ser mice was also significantly greater than the number of c-Fos-immunopositive VTA neurons in nicotine-treated control animals. In control mice, 0.09 mg/kg nicotine did not significantly increase the number of c-Fos-immunopositive VTA neurons compared to saline. To determine whether nicotine-activated neurons were predominantly non-DAergic, we challenged control and Gad2^{VTA}:Leu9′Ser mice with 0.09 mg/kg nicotine and double immunolabeled for c-Fos and TH (Fig. 2*B*,*C*). Two-way ANOVA revealed a significant main effect of virus expression ($F_{(1,22)} = 5.3$, $p < 0.05$) and neuron subpopulation ($F_{(1,22)} = 10.0$, $p < 0.01$), and a virus expression by nicotine treatment interaction ($F_{(1,22)} = 4.73$, $p < 0.05$). *Post hoc* analysis indicated that the number of TH-immunonegative, c-Fos-immunopositive neurons in Gad2^{VTA}:Leu9′Ser was significantly larger than TH-immunopositive, c-Fos-immunopositive neurons after nicotine challenge ($p < 0.01$). The number of TH-immunonegative, c-Fos-immunopositive neurons in Gad2^{VTA}:Leu9′Ser was also larger than the number of TH-immunonegative, c-Fos-immunopositive neurons in control mice after nicotine challenge ($p < 0.05$). The number of TH-immunopositive, c-Fos-immunopositive neurons in Gad2^{VTA}:Leu9′Ser mice after nicotine challenge was small and not significantly different from control mice. In addition, YFP signal could be detected in c-Fos-immunopositive neurons in Gad2^{VTA}:Leu9′Ser mice, but not in control mice (Fig. 2*B*). Together, these data indicate that 0.09 mg/kg nicotine selectively activates non-DAergic (i.e., GABAergic) neurons in Gad2^{VTA}:Leu9′Ser mice.

Nicotine activation of α4* nicotinic receptors in VTA GABAergic neurons: locomotor effects

To test the hypothesis that functional upregulation of nAChRs in GABAergic neurons may be involved in nicotine tolerance (Nashmi et al., 2007), we measured nicotine-induced locomotor activity in response to single daily injections of the drug for 7 d in Gad2^{VTA}:Leu9′Ser and control animals. Mice were challenged with 0.09 mg/kg nicotine delivered subcutaneously, a dose that activated GABAergic neurons in Gad2^{VTA}:Leu9′Ser but had little effect on neuronal activation in control mice. In control mice, 0.09 mg/kg nicotine did not significantly modulate locomotor activity compared to saline injection (Fig. 3*A*). In Gad2^{VTA}:Leu9′Ser mice, one-way ANOVA revealed a significant main effect of nicotine injections on locomotor activity ($F_{(3,18)} = 7.86$, $p < 0.01$). *Post hoc* analysis revealed that nicotine significantly depressed locomotor activity upon first injection compared to saline ($p < 0.01$), and tolerance to this hypolocomotor response

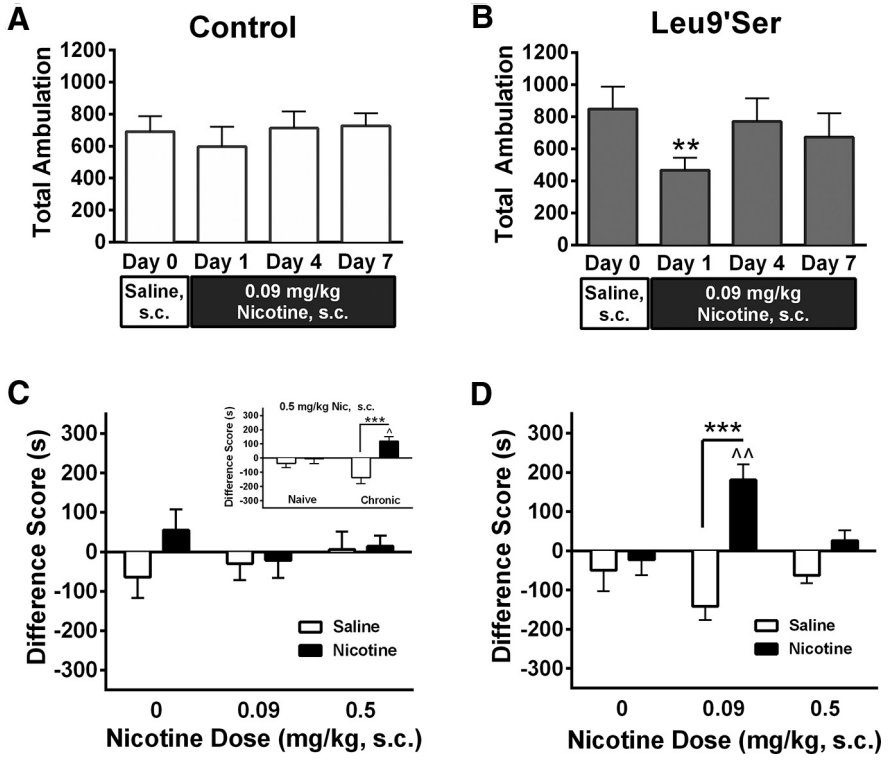

Figure 3. Selective activation of VTA GABAergic neurons by nicotine is sufficient for nicotine-induced hypolocomotion and reward. ***A***, Summed 15 min total locomotor activity after saline injection or daily injection of 0.09 mg/kg nicotine in control mice ($n = 7$). ***B***, Summed 15 min total locomotor activity after saline injection or daily injection of 0.09 mg/kg nicotine in Gad2^{VTA}:Leu9′Ser mice ($n = 7$). ** $p < 0.01$, compared to saline challenge. ***C***, ***D***, Difference scores indicate the time spent in the nicotine- or saline-paired chamber after training minus the time spent in the nicotine- or saline-paired chamber before training in control (***C***) or Gad2^{VTA}:Leu9′Ser mice (***D***) in response to 0 mg/kg (saline; $n = 10$ and 8, respectively), 0.09 mg/kg ($n = 9$/group), and 0.5 mg/kg nicotine ($n = 8$/group). ***C***, Inset, Difference scores in the CPP assay in response to 0.5 mg/kg nicotine from WT mice previously exposed to 6 weeks of nicotine or vehicle ($n = 11$/group). *** $p < 0.001$ (nicotine-paired chamber compared to saline-paired chamber); ^ $p < 0.05$ (nicotine-paired chamber in dependent mice compared to nicotine-paired chamber in nicotine-naive mice); ^^ $p < 0.01$ (nicotine-paired chamber compared to saline in the drug-paired chamber); two-way ANOVA, Bonferroni's *post hoc* test. Error bars indicate SEM.

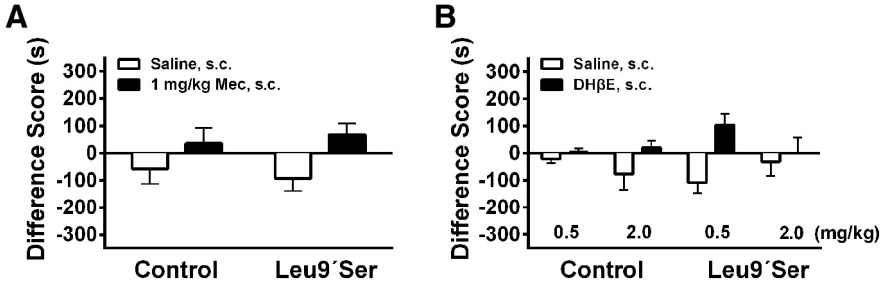

Figure 4. nAChR antagonists do not condition a place preference in Gad2^{VTA}:Leu9′Ser mice. ***A***, Difference scores in the CPP assay in response to 1.0 mg/kg mecamylamine in control and Gad2^{VTA}:Leu9′Ser mice ($n = 10$/group). ***B***, Difference scores in the CPP assay in response to 0.5 or 2.0 mg/kg DHβE in control mice ($n = 7$/group) and Gad2^{VTA}:Leu9′Ser mice ($n = 8$ and 6, respectively). Error bars indicate SEM.

occurred with subsequent injections. Thus, acute activation of nAChRs in VTA GABAergic neurons induces hypolocomotor activity, which triggers tolerance after subsequent nicotine exposures.

Sensitivity to nicotine reward is modulated by activation of VTA GABAergic α4* nicotinic receptors

To test the hypothesis that functional upregulation of VTA GABAergic neurons modulates nicotine reward, the ability of nicotine to condition a place preference in Gad2^{VTA}:Leu9′Ser and control mice was measured using the CPP procedure. During training, mice were challenged with saline or 0.09 or 0.5 mg/kg nicotine (Fig. 3*C*,*D*, Table 1), delivered subcutaneously. In control animals, nicotine did not condition a significant place preference in response to either dose (Fig. 3*C*), similar to previous reports delivering subcutaneous nicotine injections with the CPP procedure in C57BL/6J mice (Hilario et al., 2012), the background strain of the Gad2-Cre mice. However, a significant CPP in response to 0.5 mg/kg was observed in this strain during withdrawal from 6 weeks chronic nicotine treatment (Fig. 3*C*, inset; significant main effect of drug-paired chamber, $F_{(1,20)} = 5.97$, $p < 0.05$; significant drug-paired chamber by chronic treatment interaction, $F_{(1,20)} = 10.10$, $p < 0.01$; two-way ANOVA on difference scores, significant increase in difference score in the nicotine-paired chamber between nicotine-dependent and nicotine-naive mice, $p < 0.01$; Table 1). In Gad2^{VTA}:Leu9′Ser mice, two-way ANOVA of difference scores (Fig. 3*D*) indicated a significant main effect of drug ($F_{(1,26)} = 18.64$, $p < 0.001$) but not training chamber ($F_{(2,46)} = 0.6807$, $p > 0.05$), and a significant drug by training chamber interaction ($F_{(2,46)} = 7.086$, $p < 0.01$). *Post hoc* analysis revealed a significant difference between difference scores in the nicotine-paired chamber at the dose of 0.09 mg/kg, but not 0.5 mg/kg, nicotine in Gad2^{VTA}:Leu9′Ser mice compared to saline (Fig. 3*D*). Repeated measures two-way ANOVA of time spent in the drug and saline-paired chamber before and after training with 0.09 mg/kg nicotine (Table 1) did not indicate significant main effects of training or time spent in either chamber, but did reveal a significant training by chamber interaction ($F_{(1,8)} = 25.48$, $p < 0.001$). A *post hoc* test indicated a significant increase in time spent in the nicotine-paired chamber after training compared to before training. Finally, two-way ANOVA of time spent in the drug-paired chamber before and after training in Gad2^{VTA}:Leu9′Ser mice that received 0.09 mg/kg nicotine during training compared to mice that received saline in the drug-paired chamber (Table 1) indicated a significant main effect of drug ($F_{(1,15)} = 10.32$, $p < 0.01$) and time spent in the drug-paired chamber ($F_{(1,15)} = 7.97$, $p < 0.05$), and a significant interaction ($F_{(1,15)} = 13.19$, $p < 0.01$). *Post hoc* analysis indicated a significant increase in time spent in the drug-paired chamber after training with 0.09 mg/kg nicotine compared to saline. Interestingly, after chronic nicotine exposure, Gad2^{VTA}:Leu9′Ser mice did develop a modest CPP to 0.5 mg/kg nicotine (repeated measures two-way ANOVA; significant

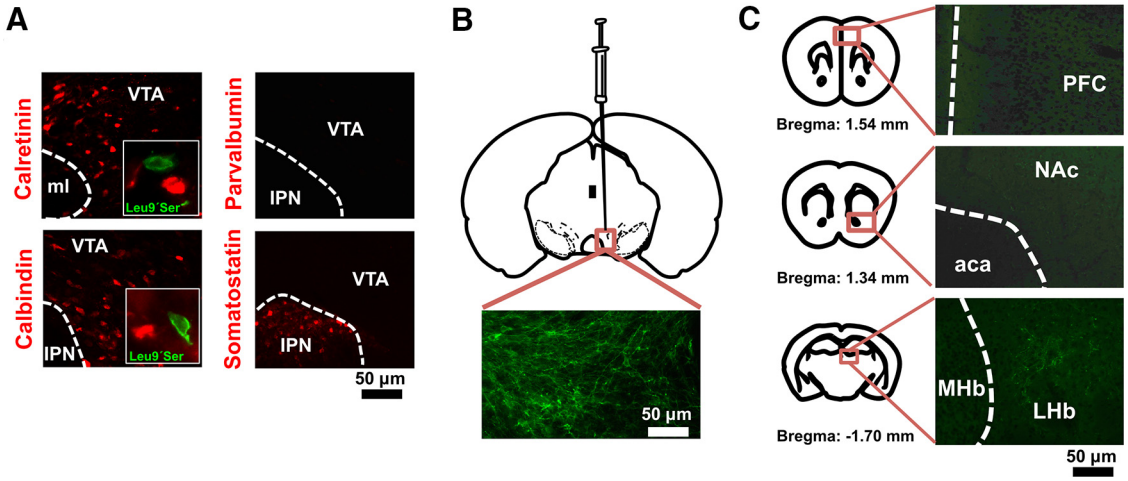

Figure 5. GABAergic neurons mediating reward in Gad2^{VTA}:Leu9′Ser mice include neurons that project to the lateral habenula. ***A***, Representative photomicrographs illustrating calretinin (top left), calbindin (bottom left), parvalbumin (top right), and somatostatin (bottom right) immunolabeling (red) in C57BL/6J midbrain sections. Insets depict distinct localization of calretinin or calbindin (red) compared to YFP expression (yellow) in Gad2^{VTA}:Leu9′Ser mice. ***B***, Depiction of a coronal section from a Gad2^{VTA}:Leu9′Ser mouse used for analysis of GABAergic projections. The photomicrograph illustrates YFP signal in the VTA. ***C***, Representative photomicrographs from cortical (top), striatal (middle), and epithalamic (bottom) sections from the Gad2^{VTA}:Leu9′Ser mouse in ***B***. IPN, Interpeduncular nucleus; ml, mammillary nucleus; aca, anterior commissure; MHb, medial habenula.

training by chamber interaction, $F_{(1,9)} = 27.61$, $p < 0.001$; significant increase in time spent in the nicotine-paired chamber after training, $p < 0.05$; Table 1).

Whereas a low dose of nicotine may elicit a CPP in Gad2^{VTA}:Leu9′Ser mice by activating GABAergic neurons, it is also possible that nicotine may be desensitizing Leu9′Ser α4-YFP nAChRs in VTA GABAergic interneurons, reducing endogenous ACh activation of the mutant nAChRs (i.e., blocking GABAergic interneuron activity) and thereby disinhibiting DAergic neurons to promote reward (Mansvelder et al., 2002). We hypothesized that if this were occurring, then an nAChR antagonist would elicit a similar effect by blocking endogenous activity through the Leu9′Ser α4-YFP nAChRs. Thus, we measured the ability of the noncompetitive nAChR antagonist mecamylamine to condition a place preference in Gad2^{VTA}:Leu9′Ser and control, nicotine-naive animals. In both groups, 1.0 mg/kg mecamylamine failed to significantly condition a place preference (Fig. 4*A*). In an additional group of Gad2^{VTA}:Leu9′Ser and control nicotine-naive animals, we tested whether DHβE, a selective α4β2 competitive antagonist, would be sufficient to disinhibit DAergic neurons and condition a place preference. Training with 0.5 or 2.0 mg/kg DHβE, subcutaneously, in control and Gad2^{VTA}:Leu9′Ser mice failed to condition a place preference (Fig. 4*B*). These data indicate that selective activation of α4* nAChRs in GABAergic neurons is sufficient for nicotine reward.

Gad2^{VTA}:Leu9′Ser mice α4* nAChRs are expressed in VTA GABAergic neurons that project to the lateral habenula

To gain insight into the neuronal subpopulation(s) of VTA GABAergic neurons that may express the Leu9′Ser α4-YFP subunit and elicit nicotine-induced reward in Gad2^{VTA}:Leu9′Ser animals, we immunolabeled C57BL/6J midbrain slices with potential GABAergic neuronal markers calretinin, calbindin, somatostatin, and parvalbumin (Fig. 5*A*). Interestingly, we did not detect somatostatin nor parvalbumin expression in the area of the VTA that was targeted with our virus expression system (that is, the posterior VTA), although somatostatin expression was observed in the rostral interpeduncular nucleus as described previously (Zhao-Shea et al., 2013). Both calretinin- and calbindin-immunopositive cells were detected (Fig. 5*A*). However, analysis of YFP signal in Gad2^{VTA}:Leu9′Ser mice revealed that calretinin- and calbindin-immunopositive neurons did not express YFP (Fig. 5*A*, insets), consistent with previous reports that the majority of calretinin- and calbindin-expressing VTA neurons are actually DAergic (Olson and Nestler, 2007). We next analyzed YFP signal in known VTA efferent brain regions of Gad2^{VTA}:Leu9′Ser mice including the NAc, prefrontal cortex (PFC), and lateral habenula (LHb), for YFP fluorescence (Fig. 5*B*,*C*). Interestingly, YFP signal was not detected in the PFC or NAc. However, fluorescence was observed in the LHb.

Discussion

We expressed Leu9′Ser α4-YFP nAChR subunits in VTA GABAergic neurons in an effort to understand how functional upregulation of α4* nAChRs in this neuronal subpopulation may contribute to behaviors associated with nicotine dependence. Chronic nicotine upregulates α4* nAChRs selectively in GABAergic neurons of the VTA, and this is accompanied by an increase in functional expression as measured by an increase in nicotine activation of these neurons (Nashmi et al., 2007). It is important to note that if chronic nicotine merely upregulated the α4 nAChR subunit and not the β2 subunit, then this would result in a change in α4β2 nAChR stoichiometry to the low sensitivity (α4)3(β2)2 subtype (Eaton et al., 2014). However, a functional increase in activation is observed in chronic nicotine-treated animals, suggesting that upregulation of both α4 and β2 subunits occurs (Srinivasan et al., 2011), leading to the observed increase in nAChR function in GABAergic VTA neurons. To mimic this phenomenon, we chose to express gain-of-function α4 nAChR subunits in GABAergic VTA neurons instead of wild-type (WT) subunits, which would have likely changed the α4β2 nAChR stoichiometry to the low sensitivity (α4)3(β2)2 subtype resulting in a loss-of-function phenotype.

In Gad2^{VTA}:Leu9′Ser mice, a low dose of 0.09 mg/kg nicotine was sufficient to activate GABAergic neurons. This same dose failed to significantly activate neurons in control animals. Interestingly, there were few DAergic neurons activated in both control and Gad2^{VTA}:Leu9′Ser mice after low-dose nicotine challenge. Importantly, nicotine was delivered subcutaneously in these experiments, whereas this same dose has been shown to

elicit reward in mice when delivered intraperitoneally, highlighting that routes of nicotine administration yield differences in bioavailability of the drug (Brunzell et al., 2009; Alcantara et al., 2014).

Acute nicotine activation of VTA GABAergic neurons induces hypolocomotion

We assessed how functional upregulation of VTA GABAergic neurons may contribute to nicotine tolerance and reward. Acute nicotine induces hypolocomotion in rodents, which is alleviated with multiple nicotine exposures, providing a behavioral measure of tolerance (Tapper et al., 2007). Typically, locomotor suppression has been observed in C57BL/6 mice given a dose of ~0.5 mg/kg nicotine in a novel environment or open field (Salas et al., 2004). A single injection of 0.09 mg/kg nicotine in a novel cage was sufficient to decrease locomotor activity in Gad2^{VTA}:Leu9′Ser mice, but had little effect on locomotor activity in control mice. Interestingly, Gad2^{VTA}:Leu9′Ser mice developed a tolerance to this effect with daily low-dose nicotine injections, indicating that acute activation of VTA GABAergic neurons induces hypolocomotion, with subsequent exposures eliciting tolerance to this effect. The mechanism underlying nicotine-induced hypolocomotor activity is unknown. Our data indicate that activation of VTA GABAergic neurons may cause the initial nicotine-induced decrease in locomotor activity perhaps by inhibiting DA release into the striatum. However, additional experiments will be needed to determine whether the tolerance to this hypolocomotion involves α4* nAChRs in GABAergic neurons or, alternatively, triggers a non-nAChR mechanism that opposes hypolocomotion.

Selective activation of VTA GABAergic neurons by nicotine is sufficient for reward

Previous studies using optogenetic stimulation have shown that activation of VTA GABAergic neurons can lead to disruption of reward and induce aversion (Tan et al., 2012; van Zessen et al., 2012). Surprisingly, selective activation of VTA GABAergic neurons in Gad2^{VTA}:Leu9′Ser mice using a low dose of nicotine conditioned a robust place preference in these animals, suggesting that nicotine activation of these neurons may be sufficient for reward. Conversely, a more typical "rewarding" dose of 0.5 mg/kg subcutaneous nicotine (Hilario et al., 2012; Smith et al., 2012) failed to elicit a place preference in Gad2^{VTA}:Leu9′Ser mice, consistent with a shift in the inverted-U-shaped dose–response curve often seen with nicotine reward and reinforcement (Picciotto, 2003). In control mice, nicotine failed to condition a place preference at any of the doses tested. While stress could be a contributing factor to lack of CPP in control animals, this is rendered unlikely because mice were habituated to handling before the beginning of the CPP assay. Our results are similar to those of Hilario et al. (2012), who demonstrated that withdrawal from chronic nicotine exposure was necessary for the expression of nicotine reward and that this is correlated with nAChR upregulation. Verifying these data, we confirmed that control mice withdrawn from chronic nicotine also exhibit a place preference with 0.5 mg/kg nicotine compared to nicotine-naive mice. Based on data indicating that (1) increased sensitivity to nicotine reward occurs after chronic nicotine exposure and withdrawal, (2) sensitivity to nicotine reward correlates with nAChR upregulation (Hilario et al., 2012), (3) upregulation of α4* nAChRs occurs selectively in VTA GABAergic neurons (Nashmi et al., 2007), and (4) selective activation of functionally upregulated α4* nAChRs in VTA GABAergic neurons elicits reward, we suggest that upregulation of α4* nAChRs specifically in VTA GABAergic neurons increases sensitivity to nicotine reward.

How might activation of GABAergic neurons by nicotine elicit reward? One possibility is that nicotine desensitizes GABAergic nAChRs, reducing GABAergic neuron activity and disinhibiting DAergic neurons (Mansvelder et al., 2002). Our data indicate that, at least using our expression system, this possibility is unlikely because (1) we did not observe increased activation of DAergic neurons (as measured by c-Fos induction) after low-dose nicotine challenge in Gad2^{VTA}:Leu9′Ser neurons, and (2) mecamylamine and DHβE failed to elicit reward in Gad2^{VTA}:Leu9′Ser mice. One caveat to these results is that disinhibition of DAergic neurons by nAChR desensitization in GABAergic neurons would require that Leu9′Ser α4-YFP nAChRs are predominantly expressed in GABAergic interneurons. In analyzing VTA neuron subpopulations in the injection area of Gad2^{VTA}:Leu9′Ser mice, which was focused on the posterior VTA, we failed to detect parvalbumin- or somatostatin-immunopositive neurons, whereas calbindin and calretinin neurons were detected, but did not colocalize with Leu9′Ser α4-YFP expression, consistent with previous studies indicating that these two populations of neurons are largely DAergic in the VTA (Gerfen et al., 1987; Olson and Nestler, 2007). A more recent study indicated that activation of GABAergic neurons via β2* nAChRs is required for DAergic neuron burst activity and nicotine self-administration (Tolu et al., 2012). Thus, nicotine activation of GABAergic neurons in Gad2^{VTA}:Leu9′Ser mice could lead to increased DAergic neuron bursting and reward. However, as indicated above, increased activation of DAergic neurons, at least with acute nicotine injections, was not observed in these animals. A third and more likely possibility is that a portion of VTA GABAergic neurons expressing Leu9′Ser α4-YFP nAChRs project to brain regions that, when inhibited, promote reward behavior. Indeed, upon analysis of known VTA projection regions, we found Leu9′Ser α4-YFP expression in the LHb. GABAergic neurons make up ~35% of VTA neurons, and although little is known about their function within the VTA (Nair-Roberts et al., 2008), previous studies indicate that a portion of VTA GABAergic neurons innervate the LHb and, when activated, elicit reward (Stamatakis et al., 2013; Lammel et al., 2015). This is accomplished by inhibiting LHb glutamatergic inputs to the rostromedial tegmental nucleus (RMTg), which, in turn, disinhibits VTA DAergic neurons to promote reward (Hong et al., 2011; Lecca et al., 2011). Thus, one mechanism by which nicotine activation of VTA GABAergic neurons could elicit nicotine reward is through inhibiting these LHb inputs to the RMTg. Future studies should focus on how VTA GABAergic neuron activation alters the excitability of these downstream brain regions in the context of nicotine-induced reward. Our data suggest that activation of functionally upregulated α4* nAChRs in VTA GABAergic neurons confers increased sensitivity to nicotine reward. These data indicate that nAChR subtypes specifically expressed in VTA GABAergic neurons may be good molecular targets for therapeutics to aide in smoking cessation.

References

Alcantara LF, Warren BL, Parise EM, Iniguez SD, Bolanos-Guzman CA (2014) Effects of psychotropic drugs on second messenger signaling and preference for nicotine in juvenile male mice. Psychopharmacology (Berl) 231:1479–1492. CrossRef

Brunzell DH, Mineur YS, Neve RL, Picciotto MR (2009) Nucleus accumbens CREB activity is necessary for nicotine conditioned place preference. Neuropsychopharmacology 34:1993–2001. CrossRef Medline

Brunzell DH, Boschen KE, Hendrick ES, Beardsley PM, McIntosh JM (2010) Alpha-conotoxin MII-sensitive nicotinic acetylcholine receptors in the nucleus accumbens shell regulate progressive ratio responding maintained by nicotine. Neuropsychopharmacology 35:665–673. CrossRef Medline

Cole AJ, Saffen DW, Baraban JM, Worley PF (1989) Rapid increase of an immediate early gene messenger RNA in hippocampal neurons by synaptic NMDA receptor activation. Nature 340:474–476. CrossRef Medline

De Biasi M, Dani JA (2011) Reward, addiction, withdrawal to nicotine. Annu Rev Neurosci 34:105–130. CrossRef

Eaton JB, Lucero LM, Stratton H, Chang Y, Cooper JF, Lindstrom JM, Lukas RJ, Whiteaker P (2014) The unique alpha4+/-alpha4 agonist binding site in (alpha4)3(beta2)2 subtype nicotinic acetylcholine receptors permits differential agonist desensitization pharmacology versus the (alpha4)2(beta2)3 subtype. J Pharmacol Exp Ther 348:46–58. Medline

Gerfen CR, Baimbridge KG, Thibault J (1987) The neostriatal mosaic: III. Biochemical and developmental dissociation of patch-matrix mesostriatal systems. J Neurosci 7:3935–3944. Medline

Gotti C, Guiducci S, Tedesco V, Corbioli S, Zanetti L, Moretti M, Zanardi A, Rimondini R, Mugnaini M, Clementi F, Chiamulera C, Zoli M (2010) Nicotinic acetylcholine receptors in the mesolimbic pathway: primary role of ventral tegmental area alpha6beta2* receptors in mediating systemic nicotine effects on dopamine release, locomotion, and reinforcement. J Neurosci 30:5311–5325. CrossRef Medline

Harris DS, Anthenelli RM (2005) Expanding treatment of tobacco dependence. Curr Psychiatry Rep 7:344–351. CrossRef Medline

Hilario MR, Turner JR, Blendy JA (2012) Reward sensitization: effects of repeated nicotine exposure and withdrawal in mice. Neuropsychopharmacology 37:2661–2670. CrossRef

Hong S, Jhou TC, Smith M, Saleem KS, Hikosaka O (2011) Negative reward signals from the lateral habenula to dopamine neurons are mediated by rostromedial tegmental nucleus in primates. J Neurosci 31:11457–11471. CrossRef Medline

Johnson SW, North RA (1992) Two types of neurone in the rat ventral tegmental area and their synaptic inputs. J Physiol 450:455–468. CrossRef Medline

Klink R, de Kerchove d'Exaerde A, Zoli M, Changeux JP (2001) Molecular and physiological diversity of nicotinic acetylcholine receptors in the midbrain dopaminergic nuclei. J Neurosci 21:1452–1463. Medline

Labarca C, Schwarz J, Deshpande P, Schwarz S, Nowak MW, Fonck C, Nashmi R, Kofuji P, Dang H, Shi W, Fidan M, Khakh BS, Chen Z, Bowers BJ, Boulter J, Wehner JM, Lester HA (2001) Point mutant mice with hypersensitive alpha 4 nicotinic receptors show dopaminergic deficits and increased anxiety. Proc Natl Acad Sci U S A 98:2786–2791. CrossRef Medline

Lammel S, Steinberg EE, Földy C, Wall NR, Beier K, Luo L, Malenka RC (2015) Diversity of transgenic mouse models for selective targeting of midbrain dopamine neurons. Neuron 85:429–438. CrossRef Medline

Lecca S, Melis M, Luchicchi A, Ennas MG, Castelli MP, Muntoni AL, Pistis M (2011) Effects of drugs of abuse on putative rostromedial tegmental neurons, inhibitory afferents to midbrain dopamine cells. Neuropsychopharmacology 36:589–602. CrossRef Medline

Mansvelder HD, Keath JR, McGehee DS (2002) Synaptic mechanisms underlie nicotine-induced excitability of brain reward areas. Neuron 33:905–919. CrossRef Medline

Maskos U, Molles BE, Pons S, Besson M, Guiard BP, Guilloux JP, Evrard A, Cazala P, Cormier A, Mameli-Engvall M, Dufour N, Cloëz-Tayarani I, Bemelmans AP, Mallet J, Gardier AM, David V, Faure P, Granon S, Changeux JP (2005) Nicotine reinforcement and cognition restored by targeted expression of nicotinic receptors. Nature 436:103–107. CrossRef Medline

Nair-Roberts RG, Chatelain-Badie SD, Benson E, White-Cooper H, Bolam JP, Ungless MA (2008) Stereological estimates of dopaminergic, GABAergic and glutamatergic neurons in the ventral tegmental area, substantia nigra and retrorubral field in the rat. Neuroscience 152:1024–1031. CrossRef Medline

Nashmi R, Dickinson ME, McKinney S, Jareb M, Labarca C, Fraser SE, Lester HA (2003) Assembly of alpha4beta2 nicotinic acetylcholine receptors assessed with functional fluorescently labeled subunits: effects of localization, trafficking, and nicotine-induced upregulation in clonal mammalian cells and in cultured midbrain neurons. J Neurosci 23:11554–11567. Medline

Nashmi R, Xiao C, Deshpande P, McKinney S, Grady SR, Whiteaker P, Huang Q, McClure-Begley T, Lindstrom JM, Labarca C, Collins AC, Marks MJ, Lester HA (2007) Chronic nicotine cell specifically upregulates functional alpha 4* nicotinic receptors: basis for both tolerance in midbrain and enhanced long-term potentiation in perforant path. J Neurosci 27:8202–8218. CrossRef Medline

Olson VG, Nestler EJ (2007) Topographical organization of GABAergic neurons within the ventral tegmental area of the rat. Synapse 61:87–95. CrossRef Medline

Picciotto MR (2003) Nicotine as a modulator of behavior: beyond the inverted U. Trends Pharmacol Sci 24:493–499. CrossRef Medline

Picciotto MR, Zoli M, Rimondini R, Léna C, Marubio LM, Pich EM, Fuxe K, Changeux JP (1998) Acetylcholine receptors containing the beta2 subunit are involved in the reinforcing properties of nicotine. Nature 391:173–177. CrossRef Medline

Pons S, Fattore L, Cossu G, Tolu S, Porcu E, McIntosh JM, Changeux JP, Maskos U, Fratta W (2008) Crucial role of alpha4 and alpha6 nicotinic acetylcholine receptor subunits from ventral tegmental area in systemic nicotine self-administration. J Neurosci 28:12318–12327. CrossRef Medline

Salas R, Cook KD, Bassetto L, De Biasi M (2004) The alpha3 and beta4 nicotinic acetylcholine receptor subunits are necessary for nicotine-induced seizures and hypolocomotion in mice. Neuropharmacology 47:401–407. CrossRef Medline

Smith JS, Schindler AG, Martinelli E, Gustin RM, Bruchas MR, Chavkin C (2012) Stress-induced activation of the dynorphin/kappa-opioid receptor system in the amygdala potentiates nicotine conditioned place preference. J Neurosci 32:1488–1495. CrossRef Medline

Srinivasan R, Pantoja R, Moss FJ, Mackey ED, Son CD, Miwa J, Lester HA (2011) Nicotine up-regulates alpha4beta2 nicotinic receptors and ER exit sites via stoichiometry-dependent chaperoning. J Gen Physiol 137:59–79. CrossRef

Stamatakis AM, Jennings JH, Ung RL, Blair GA, Weinberg RJ, Neve RL, Boyce F, Mattis J, Ramakrishnan C, Deisseroth K, Stuber GD (2013) A unique population of ventral tegmental area neurons inhibits the lateral habenula to promote reward. Neuron 80:1039–1053. CrossRef Medline

Tan KR, Yvon C, Turiault M, Mirzabekov JJ, Doehner J, Labouèbe G, Deisseroth K, Tye KM, Lüscher C (2012) GABA neurons of the VTA drive conditioned place aversion. Neuron 73:1173–1183. CrossRef Medline

Taniguchi H, He M, Wu P, Kim S, Paik R, Sugino K, Kvitsani D, Fu Y, Lu J, Lin Y, Miyoshi G, Shima Y, Fishell G, Nelson SB, Huang ZJ (2011) A resource of Cre driver lines for genetic targeting of GABAergic neurons in cerebral cortex. Neuron 71:995–1013. CrossRef Medline

Tapper AR, McKinney SL, Nashmi R, Schwarz J, Deshpande P, Labarca C, Whiteaker P, Marks MJ, Collins AC, Lester HA (2004) Nicotine activation of alpha4* receptors: sufficient for reward, tolerance, and sensitization. Science 306:1029–1032. CrossRef Medline

Tapper AR, McKinney SL, Marks MJ, Lester HA (2007) Nicotine responses in hypersensitive and knockout alpha 4 mice account for tolerance to both hypothermia and locomotor suppression in wild-type mice. Physiol Genomics. 31:422–428. Medline

Tolu S, Eddine R, Marti F, David V, Graupner M, Pons S, Baudonnat M, Husson M, Besson M, Reperant C, Zemdegs J, Pages C, Hay YA, Lambolez B, Caboche J, Gutkin B, Gardier AM, Changeux JP, Faure P, Maskos U (2012) Co-activation of VTA DA and GABA neurons mediates nicotine reinforcement. Mol Psychiatry 18:382–393. CrossRef

Tsai HC, Zhang F, Adamantidis A, Stuber GD, Bonci A, de Lecea L, Deisseroth K (2009) Phasic firing in dopaminergic neurons is sufficient for behavioral conditioning. Science 324:1080–1084. CrossRef Medline

van Zessen R, Phillips JL, Budygin EA, Stuber GD (2012) Activation of VTA GABA neurons disrupts reward consumption. Neuron 73:1184–1194. CrossRef Medline

Wonnacott S (1990) The paradox of nicotinic acetylcholine receptor upregulation by nicotine. Trends Pharmacol Sci 11:216–219. CrossRef Medline

Wooltorton JR, Pidoplichko VI, Broide RS, Dani JA (2003) Differential desensitization and distribution of nicotinic acetylcholine receptor subtypes in midbrain dopamine areas. J Neurosci 23:3176–3185. Medline

Xiao C, Nashmi R, McKinney S, Cai H, McIntosh JM, Lester HA (2009) Chronic nicotine selectively enhances alpha4beta2* nicotinic acetylcholine receptors in the nigrostriatal dopamine pathway. J Neurosci 29:12428–12439. CrossRef Medline

Zhao-Shea R, Liu L, Soll LG, Improgo MR, Meyers EE, McIntosh JM, Grady SR, Marks MJ, Gardner PD, Tapper AR (2011) Nicotine-mediated activation of dopaminergic neurons in distinct regions of the ventral tegmental area. Neuropsychopharmacology 36:1021–1032. CrossRef Medline

Zhao-Shea R, Liu L, Pang X, Gardner PD, Tapper AR (2013) Activation of GABAergic neurons in the interpeduncular nucleus triggers physical nicotine withdrawal symptoms. Curr Biol 23:2327–2335. CrossRef Medline